



Research Article

ISSN : 0975-7384
CODEN(USA) : JCPRC5

Research on medical image fusion based on improved redundant complex wavelet transform

Tang Yong-Zheng

The Modern Educational Technology Center of Yancheng Institute of Technology, Yancheng, China

ABSTRACT

Medical image fusion refers to the process of information integration for several medical images in the same scene. The result medical image from fusion will describe the scene in a more accurate manner than any other single medical images. The paper proposes a multi-focus medical image fusion method which integrates the traditional fusion based on pixels and characteristics. Firstly, it decomposes multi-focus medical image fusion redundant wavelet transform (RWT). Then, it uses the extracted brink features to guide the organization coefficient. Finally, it uses RWT inverse transformation to reconstruct fusion medical image. According to experimental result of several multi-focus medical image fusion, the fusion method proposed by the paper shows better fusion effect than the gradient pyramid transformation and non-consecutive wavelet transformation.

Key words: Multi-focus, Medical image Fusion technology, Redundant Complex Wavelet Transform

INTRODUCTION

Medical imaging has become an essential part of modern medicine, which runs through the whole clinical work. The results of medical imaging can offer the effective basis for choosing the proper pharmacy. The medical image can be divided into two parts, which are anatomical image and functional image, The anatomical image can describe the Human body information, which concludes the X ray imaging, CT, MRI, US, and sequence diagram obtained from endoscope. The functional image can describe the metabolic information of human body, which concludes EEG, MEG, FCT and so on.

The information provided by many imaging modes are mutual in function, in order to apply many imaging modes and offer the entire information, it is necessary to intergrate the effective information. The first step of integrating the images is to make the geometric arrangement of many images exactly correspond each other in space domain, This step names as "registration". The second step of integrating the images is to show the intergrated information after the first step is over, this step names as "fusion".

Medical image fusion refers to a branch of data fusion. It refers to a process of fusion itself into a synthetic medical image so as to obtain more information or become more suitable for visual sense and computer process through processing the organized information from two or more original medical image in the same scene. Recently, medical image fusion has been widely applied to areas such as remote control, medical imaging, micro-scope imaging, robot, etc. For example, a good fusion mechanism could extract the spatial information of full colour medical images while maintaining the characteristic of band in the frequency domain to strengthen space multi-spectral medical image. The method is named Pan Sharpen. The result is shown in figure 1. Or one could extract the focus part from the multi-focus fusion medical image to form the focus medical image, as shown in figure2. The later application of this technology is named multi-focus medical image fusion.

An effective RWT-based multi-focus medical image fusion algorithm is put forward in this research. This algorithm combines pixel-level medical image fusion and feature-level medical image fusion in some aspects. First, edge features are extracted from wavelet domain of each input medical image, and then according to the edge feature, the characteristics of the response or establishment of decision diagrams in the activity area guide the RWT domain medical image fusion process. As the edges of objects and parts of objects contain the information that we are interested in, we should concentrate fusion algorithm on these areas. Different fusion results of visual and quantitative analysis confirmed that the proposed approach improves fusion quality and is better than some of the pixel-based fusion methods.

Proposed scheme

(1) Fusion Plan

This divide obtains approximate coefficients of sub band through a low-pass filtering $b(n)$ and scaling function $\varphi(x)$ applications:

$$a_j(k) = \sum_n b(n)a_{j-1}(k + n2^{j-1}), j = 1, \dots, N \quad (1)$$

Here $a_0(k)$ refers to the original discrete signal $s(k)$; j and N refer to scaling mark and scaling parameter. The follows are similar.

Wavelet coefficient could get the following formula through high pass filtering and wavelet function $\psi(x)$ application:

$$\omega_j(k) = \sum_n g(n)a_{j-1}(k + n2^{j-1}) \quad (2)$$

The data perfect reconstruction (PR) can complete the two double filter $br(n)$ and $gr(n)$ realization by meeting the conditions of quadrature mirror filter

$$\sum_n br(n)b(l-n) + gr(n)g(l-n) = \delta(l) \quad (3)$$

Here $\delta(l)$ refers to Dirac function.

A simple method of selection of $br(n)$ and $gr(n)$ can consider the equality between $br(n)$ and $gr(n)$ on one hand and $(br(n) = gr(n) = \delta(l))$ on the other. Thus through formula (3), $g(n)$ could be simplified as:

$$g(n) = \delta(n) - b(n) \quad (4)$$

Therefore, wavelet coefficient could be obtained simply with the difference between two subband approximate coefficient as shown by formula (5):

$$\omega_j(k) = a_{j-1}(k) - a_j(k) \quad (5)$$

Use convolution operation of filter and scaling function to create number. If medical image I is given, the approximate coefficient of the number could be created through the following formula:

$$A_1 = F(I), A_2 = F(A_1), A_3 = F(A_2), \dots \quad (6)$$

Here, F indicates the scaling function. A refers to the cubic spline function of B3. Usually, it is used to indicate the scaling function. Meanwhile, the application of the cubic spline function of B3 could obtain a 5×5 convolution operation module.

$$\frac{1}{256} \begin{bmatrix} 1 & 4 & 6 & 4 & 1 \\ 4 & 16 & 24 & 16 & 4 \\ 6 & 24 & 36 & 24 & 6 \\ 4 & 16 & 24 & 16 & 4 \\ 1 & 4 & 6 & 4 & 1 \end{bmatrix} \quad (7)$$

As the abovementioned situations, wavelet plane calculate with two continuous approximate coefficients A_{j-1} and A_j . Order

$$d_j = A_{j-1} - A_j, j = 1, \dots, n \quad (8)$$

where $A_0 = I$, reconstructed equation is:

$$I = \sum_{j=1}^J d_j + A_J \quad (9)$$

In the equation, $A_j (j = 0, 1, \dots, J)$ is the approximate coefficient of original medical image I under the situation when scale increases (lower the resolution level). $d_j (j = 1, \dots, J)$ refers to multi-resolution wavelet plane and A_J refers to after medical image.

It is noted that the original medical image A_0 is twice the resolution of the medical image A_1 , which is twice the resolution of the medical image A_2 , and so on. However, all the successive approximation coefficient (and wavelet plane) in the processing as compared with the source medical image contains the same pixel which makes the 'à trous' algorithm become Philippine orthogonal oversampling transformation.

In this section, the paper proposed a new algorithm which combined pixel-level and feature-level fusion method for multi-resolution medical image fusion. The basic idea is through the RWT method to extract edge features, and then use these features to guide the combination process. As the middle of the process from pixel-based fusion to feature-based fusion, this approach is more robust and overcomes defects that some known pixel level fusion algorithm is highly sensitive to noise and uncalibrated areas.

The overall flow diagram of this fusion method is shown in Figure 3. The input medical image must be pre-calibrated and the corresponding pixel through alignment. First, decompose the X and Y of the source medical image with 'à trous' algorithm, and through a series of wavelet coefficient sets each medical image. Then decomposed medical image through the fusion rules is reconstructed. Finally, retain through the inverse transform by RWT and the fused medical image Z .

(2) Feature Extraction: Brink Detail Enhancement

The dramatic changes in the intensity of the point are often the edge point which contains important visual feature information. Taking into account the multi-resolution medical image edge details that have been blurred we introduce edge feature. The wavelet transform is a powerful tool for multi-scale edge detection. Undecimated 'à trous' wavelet transformation allows medical images to be decomposed into non-consecutive high-frequency information in the frequency domain where the information possesses band-pass channel without loss of high frequency information corresponding to the details of the spatial domain, such as the edge information. In the mentioned fusion method, the source medical image through 'à trous' algorithm is decomposed into wavelet plane. These wavelet plane edge features can be preserved in each layer. Absolute maximum value of the wavelet plane coefficient is applied to describe the main characteristics of the source medical image. Extracted edge details can be obtained by simple superposition of these wavelet planes. The tests show that the sum of wavelet planes could best represent the edge information. These superimposed outputs of the process are an edge medical image, which we call the edge detail enhancement (EED). According to the formula (9), the medical image I EED may be expressed as

$$EED = \sum_{j=1}^J d_j = I - A_j \quad (9)$$

Figure 1 shows a tested medical image which has been through three-layer decomposition.



Figure 1 Testing medical image and its EED

(a) Testing medical image (b) high-level decomposed medical image d3 (c) medical image remaining difference

Fusion quality depends on the choice of the appropriate fusion rules. In the new method mentioned in this article, the medical image edge feature, EED, could be extracted from each piece of source medical image by 'a trous' wavelet transform. EED method only refers to the simple superposition of the wavelet plane, so this method only emphasizes the strong edge. Some important details, such as thin lines or weak edge will be ignored. Given the fluctuations in the plane of each layer wavelet coefficients in the vicinity of the zero-mean, we can realize it through EED. Therefore, the Laplacian, i.e. the second derivative, can be used to enhance each floor gradation level changes, especially near the edge changes. The Laplacian operator will generate a strong response to the details, and therefore is more suitable than the gradient operator for medical image enhancement.

Sampling metric of each medical image may be through a process called the measure of the activity metrics. Activity measurement depends on the nature of each piece of the source medical image and unique fusion algorithm. Here, we define the activity from the feature level, that is, EED, representing the main characteristics of the information. In position of the X (or Y) p of the medical image, the activity can be measured by Laplacian operator. Calculation is shown as follows:

$$L_{EED_X}(p) = \sum_{\substack{q \in R \\ q \neq p}} [EED_X(q) - EED_X(p)] \quad (10)$$

Where R refers to the domain of medical image X at the position p, q refers to the area within R. Considering more information, smooth and more robust active function LA is used to calculate the average of the following area:

$$LA_x(p) = \left| \frac{1}{n_w} \sum_{q \in W} L_{EED}(q) \right| \quad (11)$$

Where W refers to the are with the size of $m \times n$ whose center is located in p,q refers to a coefficient belonging to W. n_w refers to the number of coefficient of W. In the paper, area refers to the 5×5 area whose center is located in p, so n_w stands at 25.

(3) Decision Figure

The decision figure building is the key, because its output determines the synthesis figure. Therefore, the decision figure determines the different combination and decomposition of the wavelet and the reconstruction of the decomposition.

In our experiments, the decision figure with the same size of the wavelet plane selects through outcome of the comparison of different actives. The selection rules are:

$$DM(p) = \begin{cases} 1 & \text{if } LA_x(p) > LA_y(p) \\ -1 & \text{if } LA_x(p) < LA_y(p) \\ 0 & \text{if } LA_x(p) = LA_y(p) \end{cases} \quad (12)$$

Decision map is pretreated by the formula (13), because decisions only selected coefficient without introducing neighborhood reference. Some people think that space short-distance sampling might belong to the same medical image feature, and therefore can be processed by the same method. When comparing corresponding medical image features of multi-source medical image and consider the determinants of transformation coefficients, one may find a more robust fusion strategy. Li and others simplify the decision figure and prove the conformity of medical images with master figure filter. Especially when the center decomposition coefficient is from medical image X and neighboring decision-making factor is derived from the medical image Y, center sampling points become from the medical image Y. The consistency verification methods streamline the prior decision map, so as to obtain a new decision diagram map (NDM). Therefore, the composite medical image Z is ultimately obtained based on NDM.

$$\begin{cases} d_{j,z}(p) = d_{j,x}(p), j = 1, \dots, J \\ A_{j,z}(p) = A_{j,x}(p), j = J \end{cases} \quad \text{if } NDM(p) = 1$$

(13)

$$\begin{cases} d_{j,z}(p) = d_{j,y}(p), j = 1, \dots, J \\ A_{j,z}(p) = A_{j,y}(p), j = J \end{cases} \quad \text{if } NDM(p) = -1 \quad (14)$$

$$\begin{cases} d_{j,z}(p) = [d_{j,y}(p) + d_{j,x}(p)] / 2, j = 1, \dots, J \\ A_{j,z}(p) = [A_{j,y}(p) + A_{j,x}(p)] / 2, j = J \end{cases} \quad \text{if } NDM(p) = 0 \quad (15)$$

Since the decision map is constructed based on the edge features, these decision-making methods attempts to find a representative medical image feature, namely edge space and changes of space and scale are stable. Once the decision map is identified, it is applicable to all the wavelet coefficients. Here, all of the sampling points are fused by the same decision.

Firstly, evaluation standard is the mutual information (MI). It is a measure of the mutual information of the original medical image and the fusion medical image. Consider two source medical images of X, Y, and the fused medical image Z:

$$I_{Z,X}(z, x) = \sum_{z,x} P_{Z,X}(z, x) \log \frac{P_{Z,X}(z, x)}{P_Z(z)P_X(x)} \quad (16)$$

$$I_{Z,Y}(z, y) = \sum_{z,y} P_{Z,Y}(z, y) \log \frac{P_{Z,Y}(z, y)}{P_Z(z)P_Y(y)} \quad (17)$$

where P_X, P_Y, P_Z refer to the probability intensity function of medical image X, Y and Z. $P_{Z,X}, P_{Z,Y}$ refer respectively to the joint probability intensity distribution functions. So, medical image fusion result could be evaluated by formula 18:

$$MI = I_{Z,X}(z, x) + I_{Z,Y}(z, y) \quad (18)$$

The second evaluation standard refers to space frequency. It is the total measurement of the medical image in the activity layer and reflects the changes of details and textures. As for an medical image T with $m \times n$, SF could be expressed as:

$$SF = \sqrt{(RF)^2 + (CF)^2} \quad (19)$$

RF and CF refer to behavior frequency and line frequency.

$$RF = \sqrt{\frac{1}{mn} \sum_i^m \sum_j^n [T(i, j) - T(i, j-1)]^2} \quad (20)$$

$$CF = \sqrt{\frac{1}{mn} \sum_j^n \sum_i^m [T(i, j) - T(i-1, j)]^2} \quad (21)$$

As for the two principles, the bigger the numerical value, the better the fusion effect.

RESULTS AND DISCUSSION

The fusion process is completed through the following steps:

Step 1: adopt 'a trous' wavelet transformation method to the original medical image X and Y so as to decompose to the fifth layer.

Step 2: extract the medical image edge feature within the wavelet plane to obtain the edge medical images EED_X and EED_Y .

Step 3: measure and compare the active factor construction decision map of the two edge medical images.

Step 4: adopt consistency prove method to simplify the decision map and establish the synthetic medical image.

Step 5: carry out RWT inverse transformation to obtain the fusion medical image.

The proposed method has been tested in some multi-focus medical image. There are three examples given to show the effect. In the examples, the gray level is 0-255. Assume that all of the medical images have been calibrated and with no other pre-processing.

Example 1 is shown in Figure 6, which contains 9 medical images. Figure 6 (a) and (b) refer to two multi-focus medical images of different focal lengths. Only the alarm clock is properly focused. In Figure 6 (c), the decision map shows the wavelet coefficients generated from the two input medical images. The high brightness value of pixels indicates that the coefficient is from the medical image (a); the black pixels indicate it is from medical image (b). Figure 2 (d) is a fusion result using the present method. Figure 2 (e) refer to the fusion results, which adopt gradient change of pyramid, DWT method. In order to better compare the results, the original medical image and the fusion medical image are shown in Figure 6b-K. For the focus region, the source medical image and the fusion medical image should have no difference. For example, the left side of the alarm of Figure 2 (a) is clear. Figures 2d

and 2a have less difference in the left alarm compared with Figure 6b. This means that the entire focus area has been successfully included in the fused medical image. However, 6i-k in the same area have more differences, which indicates that fusion results of application of GPT, and DWT methods are worse compared with the proposed method. The same result can be attributed to our proposed method which it has better performance than the other three methods. For further comparison, we use two types of objective evaluation criteria for evaluation.

Explained the value of MI and SF in figure 2 is listed in table 1. Through MI and SF's numerical value, one could easily identify that the method we proposed is better than the other three methods. Combining the visual effect with quantifying result, the conclusion could be drawn that the fusion method proposed by the paper is better.

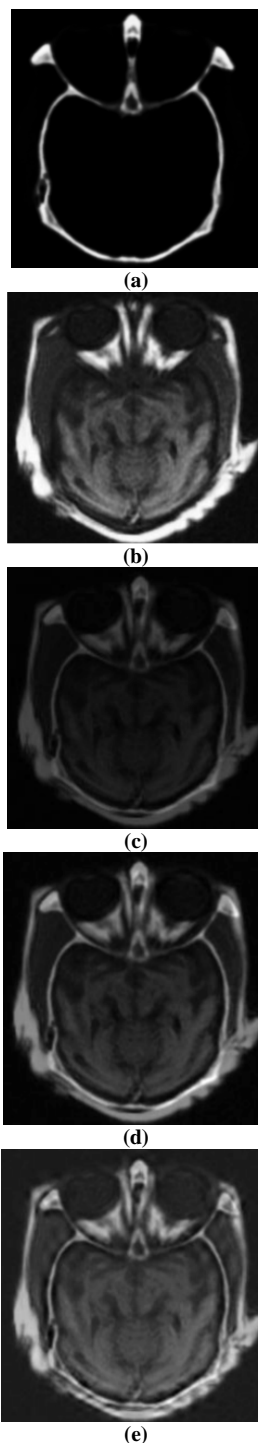


Figure 2 Test result

(a) CT Medical image (b) MRI Medical image (c) Focus Result by the Method in this Paper (d) Fusion Result by the Method of GPT (e) Fusion Effect by the Method of DWT

CONCLUSION

This research proposed multi-focus medical image fusion method combining with pixel-level fusion and some feature-level fusions based on RWT. The advantages are: (1) RWT is translation invariant, while 'a trous' algorithm has the simpler computation complexity, thus making the 'a trous' algorithm is more easily implemented thanMRA. (2) Features of pixel-level fusion, such as sensitivity to the noise, fuzzy effect and inaccuracy, have been improved. (3) The employment of features for expressing the medical image, not only reduces the complexity in the process, but also enhances the stability of the fusion result. The basic thought of this method is firstly to conduct the wavelet transformation decomposition of the 'a trous' to the input medical images, and then guide the fusion coefficient using the extracted edge feature by the wavelet plane. The fusion results of groups of multi-focus medical images show that this method produces a better result.

REFERENCES

- [1] K Vladimir; K Egiazarian; Jaakko Astola, *Journal of Mathematical Imaging and Vision*, **2002**, 6(3), 223-235.
- [2] MS Kother; SA Perumal; MM Sathik, *International Journal of Computer Science and Network Security*, **2008**, 8(1), 213-216.
- [3] B Tyler, *Applied surface science*, **2003**, 20(3): 825-831.
- [4] D Wei; SL Yu; S Sun, *Acta Electronica Sinica*, **2007**, 35(10), 1939.
- [5] Alexander, M. E., et al. "Wavelet domain de-noising of time-courses in MR medical image sequences." *Magnetic resonance imaging* 18.9 (**2000**): 1129-1134.
- [6] B Vittoria; D Vitulano, *Signal Processing*, **2006**, 86(4): 859-876.
- [7] D Ioannis; O Hammad; RI Kitney, *Physics in Medicine and biology*, **2007**, 52(13), 3741.
- [8] F Shachar; I Drori; D Cohen-Or, *ACM Transactions on Graphics (TOG)*, **2003**, 22(3), 112-116.
- [9] Deasy, Joseph O., M. Victor Wickerhauser, and Mathieu Picard. "Accelerating Monte Carlo simulations of radiation therapy dose distributions using wavelet threshold de-noising." *Medical physics* 29 (**2002**): 2366.
- [10] K Nick, *Applied and computational harmonic analysis*, **2001**, 10(3), 234-253.
- [11] YJ Yan; LA Osadciw; L. Hall, *Proceedings of CISS*, **2005**, 5(1): 45-49.
- [12] JP Dron; F Bollaers, *Journal of Sound and Vibration*, **2004**, 270(1), 61-73.
- [13] MM Guo, *Journal of Chemical and Pharmaceutical Research*, **2013**, 5(12), 64-69.
- [14] Y Qiang; YB Ma; JJ Zhao; J Wang, *Journal of Chemical and Pharmaceutical Research*, **2015**, 5(12), 183-187.